Group size dependent benefits in microbe cooperation

Author: Daniel Cornforth

Supervisor: Sam Brown

This thesis is dedicated to my mother, for constant love and support.

Acknowledgments

Firstly I'd like to thank collaborators David Sumpter and Åke Brännström who initially got me interested in game theory and adaptive dynamics and Ben Raymond who's increased my interest in infection biology. Also thanks to the various people who made me feel at home during my time at Oxford including Jay Biernaskie, Greg Wyatt, João Alpedrinha, Pauline Scanlan, Tiffany Taylor, Freya Harrison, Kevin Foster, Antonio Rodrigues, Lee Henry, Wook Kim, Lorenzo Santorelli, Natalie Jiricny, Dominic Nguyen, and Erica Machulak. Particularly thanks to my supervisor Sam Brown and my co-supervisor Angus Buckling for guidance and support.

Declaration

Chapter 1

The simplest version of the model (equation 1) and basic results in equations 2 and 3 were completed during my undergraduate degree before I began at Oxford. The rest, including the derivation of and analysis with assortment, density-dependent regulation, all figures, and the writing of the manuscript are new and were done by me at Oxford. A version of this has recently been published in the American Naturalist (Cornforth et al., 2012). Other authors helped in guidance, editing the draft and verifying analysis.

Cornforth, D.M., Sumpter, D.J., Brown, S.P., Brännström, A., 2012. Synergy and group size in microbial cooperation. The American Naturalist 180, 296.

Chapter 2

In doing work in the previous chapter, I became interested in related issues on dose-response curves. Though this did not end up in the manuscript above, it led to a collaboration with Ben Raymond who researches *Bacillus thuringiensis*. The data in this chapter (some of which is preliminary), was not collected by me, but rather by Ben Raymond and Andrew Matthews at Royal Holloway, University of London. I did the analysis, and the chapter was written by me.

Group size dependent benefits in microbe cooperation

Daniel Cornforth

St. Anne's College

MSc by Research, Michaelmas 2012

Abstract:

Microbes produce many molecules that are important for their growth and development, and the production and exploitation of these public goods has become an important paradigm in the field of microbial social evolution. Here I explore this type of microbial sociality in two primary chapters.

In the first chapter I focus on the relationship between the shape of the benefit curve and cellular density with a model assuming three types of benefit functions: diminishing, accelerating, and sigmoidal (accelerating then diminishing). I classify the latter two as being synergistic and argue that sigmoidal curves are common in microbial systems. Synergistic benefit curves interact with group sizes to give very different expected evolutionary dynamics. In particular, whether or not and to what extent microbes evolve to produce public goods depends strongly on group size. This synergy can create an ``evolutionary trap" which can stymie the establishment and maintenance of cooperation. By allowing density dependent regulation of production (quorum sensing), this trap may be avoided.

In the second chapter I focus again on group size benefits, but with a particular focus on pathogen risk assessment. Many pathogens are thought to behave collectively, and yet the models used in assessing microbial risk assume otherwise. In particular the dominant paradigm, articulated in the Independent Action Hypothesis, is that infecting microorganisms do not interact with each other and that each cell has an independent likelihood of causing infection. Initial data from a bacteria-insect system suggest that indeed the Independent Action Hypothesis may be incorrect and leads to poor risk assessment at low doses. I argue that more attention to mechanisms of infection is essential for accurate risk assessment.

Chapter 1: Synergy and group size in microbial cooperation

Introduction

Cooperative behaviour is a ubiquitous feature of interactions at all levels of biology, and a large body of theory has been developed to explain the apparent paradox of its evolution and maintenance in the face of noncooperative social cheats (e.g. Smith and Szathmáry 1995; Keller 1999; West et al. 2006). Over the past decade, microbes have proven effective in testing this theoretical work. They reproduce very quickly and are relatively easy to control and genetically manipulate. They have been used to elucidate major parts of social evolution theory like the evolution of altruism and spite and to support related evolutionary hypotheses (Griffin et al. 2004; Gardner et al. 2004; West et al. 2006). Additionally, microorganisms are fascinating in their own right and understanding their sociality carries major health consequences (Brown et al. 2009).

In microbes, among the social traits most studied is production of secreted compounds, for example compounds that scavenge for iron when iron is limited (Griffin et al. 2004) or those that convert sucrose to glucose when glucose is limited (MacLean and Gudelj 2006; Gore et al. 2009). Investigation in the past decade has only scratched the surface of these public goods, and the list of known public goods products is quickly growing (West et al. 2006). Most of this work focuses on Hamilton's rule ($rb > c$) as the condition that favors the evolution of social traits. There has been a primary focus on population structuring (shaping

Hamilton's r), though all three quantities are essential in social evolution (West et al. 2006).

In this paper, we primarily focus on fitness effects (shaping Hamilton's b and c) and specifically the group-beneficial traits of public goods production. Figure 1A shows three plausible benefit functions: one decelerating, one accelerating, and one sigmoidal (first accelerating then decelerating). We use "synergy" to refer to acceleration in benefit functions, which corresponds to the first part of the sigmoidal function and all of the accelerating function in figure 1A. This synergy allows per-capita fitness benefits to increase with group size as shown in figure 1B, sometimes termed "group augmentation" (Kokko et al. 2000). Synergy is abundant in biology, from ant pheromone trails to human architecture (Clutton-Brock 2002; Sumpter and Brännström 2008; Sumpter 2010). The mechanisms causing this synergy vary widely (Sumpter and Brännström 2008). Despite the abundance of synergy in other cooperative organisms, the phenomenon is not well-investigated in microbes. Though recent work has uncovered benefit nonlinearities in *Myxococcus* and an engineered *E. coli* system (Smith et al. 2010; Chuang et al. 2010), it is generally ruled out in mathematical models (West and Buckling 2003; Foster 2004; Ross-Gillespie et al. 2009), and the scope and impact of these nonlinearities has not been well investigated. Here we argue that although its sources and abundance are still not well understood, synergy is likely to be a key factor in microbe evolution.

Synergy occurs any time each additional public goods molecule produced gives a greater fitness benefit than the previous. Many biological molecules themselves can provide benefits in a sigmoidal fashion due to 'positively cooperative reactions" (Hill 1910). Aside from basic molecular properties, sigmoidal benefits are often expected due to ecological interactions.

For instance, the normal lifecycle of many invading parasites requires production of threshold quantities of toxins to function and/or to be able to overwhelm the immune system (Williams et al. 2000). Synergy may also arise from less apparent and more complex ecological interactions. For example, an adversarial molecule which, up to some point neutralizes produced public goods, could lead to synergy. For example, plants that produce "quorum quenching" molecules which neutralize quorum sensing molecules (whose production is, itself, cooperative (Diggle et al. 2007)). Synergy could even be caused by the consumption of others' public goods, as in, for example, the siderophore pyoverdine secreted by *Pseudomonas aeruginosa* (Brown and Kümmerli 2010).

Most theoretical studies of co-operative microbial interactions typically preclude synergy (Brown and Johnstone 2001; Foster 2004; West and Buckling 2003; Ross-Gillespie et al. 2009). It has previously been concluded that high density is disfavorable for public goods cooperation because a producing cell enjoys a growth benefit proportional to the average production of its neighbors, allowing nonproducers more opportunities to exploit high-producing cells (Ross-Gillespie et al. 2009). As we shall see here, the opposite conclusion is possible when synergy exists. Synergy has been studied previously theoretically in other contexts where an individual is classified as either a cooperator or defector (Queller 1985; Archetti 2009a,b) and more recently in a continuous-trait model (Deng and Chu 2011); see Archetti 2009b for a review on nonlinear public goods games in biology. Here, we extend these studies to continuously variable traits to understand aspects of evolution not examined in previous frameworks. We show that synergy often permits an evolutionary repellor near non-production which can have important consequences and demonstrate the role quorum sensing may play in its avoidance.

If the fitness effects of public goods production depend on density, then this should provide evolutionary pressure for microbes to regulate their production accordingly. By releasing autoinducer molecules, a cell can assess how many other cells surround it, a proxy for cellular density, and can up-regulate or down-regulate various genes in response (Fuqua et al. 1996; Robson et al. 1997). This mechanism, known as quorum sensing, regulates the expression of many genes for the secretion of extracellular molecules. In this paper, we also investigate the co-evolution of quorum sensing and a synergistic trait.

Model

We adopt a standard setting for studying games with continuous cooperative investments (Doebeli et al. 2004). We consider an infinite population, in which each individual i has a strategy or trait value x_i which represents the individual's level of cooperative investment. For simplicity, we will assume that individual cooperative investments are constrained between 0 and 1, i.e. $0 \leq x_i \leq 1$. The demographic dynamics unfold in discrete generations. At each generation, groups of size N are randomly formed. Assuming that the players in one of these groups have the respective strategies $x_1, \ldots, x_N$, the payoff for an individual i in the group, $1 \leq i \leq N$, is given by:

$$\frac{B\left(x_1+\ldots+x_N\right)}{N} - C\left(x_i\right). \tag{1}$$

Here, $B(x_1+\ldots+x_N)$ is the *collective benefit* of the group's cooperative investment (fig. 1A). The collective benefit is divided equally among the N individuals in the group to give the per-capita benefit (fig. 1B), and $C(x_i)$ is the cost of the investment. Both the benefit and cost functions are assumed strictly increasing.

The selection gradient

$$D(x) = \frac{B'(Nx)}{N} - C'(x), \tag{2}$$

indicates the direction of gradual evolutionary change in a monomorphic population of individuals all having the same trait value x, where primes denote first derivatives. For details on how the selection gradient is derived from the demographic model and how it relates to gradual evolutionary change, see Geritz et al. (1997); Sumpter and Brännström (2008); Doebeli et al. (2004); Dieckmann and Law (1996). With small mutational steps, the evolutionary dynamics will proceed in the direction indicated by the selection gradient and will cease only at a boundary strategy or at an interior strategy x^* at which the selection gradient vanishes, $D(x^*) = 0$. Such strategies are said to be evolutionarily singular. If nearby monomorphic populations evolve towards the singular strategy, it is said to be convergence stable. A convergence stable singular strategy can either be evolutionarily stable (then called continuously stable), effectively an endpoint of evolution, or it can be an evolutionary branching point at which a monomorphic population may gradually diverge to become dimorphic (Geritz et al. 1997). Mathematically, the requirement that a singular strategy is convergence stable but not evolutionarily stable can be written:

$$B''(Nx^*) < C''(x^*) < B''(Nx^*)/N < 0, \tag{3}$$

where double primes denote second derivatives. We refer to Doebeli et al. (2004); Geritz et al. (1997) for details. In words, this condition implies that both the benefit function B and the cost function C need to be decelerating in the vicinity of the singular strategy x^*.

Group size has been considered previously as the number of founders initiating a microbe colony (see Brännström and Dieckmann 2005; Brännström et al. 2010), but our analysis takes N to be the size of the group of interacting cells or neighboring bacteria within a public good molecule's radius of diffusion, which will often be a proxy for cellular density. To consider impacts of genetic assortment, we suppose that when a focal individual joins a group at the beginning of a generation, some positive fraction of the other individuals in the group may be identical to it by descent. This fraction is a random variable ρ. We show in Online Appendix A1 that, with these assumptions, the selection gradient takes the form:

$$D(x) = \frac{B'(Nx)(1+\langle\rho\rangle(N-1))}{N} - C'(x), \tag{4}$$

where brackets indicate the expectation. The condition for convergence stability is:

$$B''(Nx^*)(1+\langle\rho\rangle(N-1)) - C''(x^*) < 0 \tag{5}$$

and the criterion for evolutionary stability is:

$$\frac{B''(Nx^*)}{N}[(1+(N-1)\langle\rho\rangle)^2 + \mathrm{Var}(\rho)(N-1)^2] - C''(x^*) < 0. \tag{6}$$

Again, both the benefit function B and the cost function C need to be decelerating in the vicinity of the singular strategy x^* for evolutionary branching to occur. Interestingly, we see that the mean of ρ (which is simply others-only relatedness, see Online Appendix) is sufficient to define convergence stability, but both its mean and variance are required for evolutionary stability. Higher variance in ρ makes conditions for evolutionary branching more restrictive.

We also consider the effects of group size-dependent regulation (quorum sensing) on the maintenance of cooperation. Here an individual can alter its behavior, dependent on the size of its group. At sufficiently low group sizes, the public good is not produced, or produced in very little quantity, whereas at sufficiently high group sizes, production is simply the productive investment x. The payoff to individual i with trait values (x, s) in this model variant is simply:

$$\frac{B\left(Q(s_1,N)x_1+\ldots+Q(s_N,N)x_N\right)}{N}-C\left(Q(s_i,N)x_i\right) \tag{7}$$

where $Q(s_i,N)=1/(1+e^{s_i-N})$. Here s_i determines the group size threshold above which individual i produces public goods and below which does not (see the Online Appendix for further details).

Results

We begin by assuming that groups are formed entirely randomly among the whole population, so that there is no correlation among phenotypes of group members. Figure 2A shows the evolutionary dynamics under small mutational steps when the benefit is a decelerating function of the group's total cooperative investment (dotted line in fig. 1; diminishing returns, see also Foster 2004). Here per-capita benefits decrease with group size. Assuming that the cost is proportional to the investment $C(x)=cx$, it follows that the selection gradient $D(x)=B'(Nx)/N-c$ is strictly decreasing with x, so there is exactly one continuously stable strategy (both convergence stable and evolutionarily stable) which is either full defection, an intermediate level of cooperation, or full cooperation (fig. 2A). This CSS, once reached, is resistant to invasions by mutants with phenotypes sufficiently close on either side. This is very much the standard picture of evolutionary games involving costs and benefits to cooperation; the evolutionarily stable cooperative investment decreases with group size N (Ross-Gillespie et al. 2009).

Whereas figure 2A illustrates the implications for the most common assumptions on benefit functions, it is not necessarily the case that increasing total producers leads to decreasing per-capita benefits. The alternative scenario is where the per-capita benefit derived from cooperative interactions increases with group investment (fig. 2B). Here, for linear cost functions, the selection gradient $D(x)$ is strictly increasing and there is either one or two convergence stable strategies, corresponding to no cooperative investment or full cooperative investment. Typically, for small groups, no investment is the only evolutionarily stable strategy, but at some critical group size full investment also becomes stable (fig. 2B).

In a biologically realistic setting, synergistic interactions cannot continue indefinitely and there is a critical level at which the per-capita benefit of additional cooperative investment begins to decrease. This leads to a sigmoidal form of the benefit function B. In this situation, the evolutionary dynamics can incorporate elements of both cases discussed above. This can be seen in figure 2C where we have two branches of singular strategies; the lower is repelling (since it comes from the synergistic lower part of the benefit function), and the upper branch is attracting (due to decelerating portion of the benefit function at higher cooperative investments). In this example, cooperation first becomes possible at intermediate sizes, and then suddenly shifts to no cooperation at high group sizes.

Thus far, we have assumed that costs are proportional to the amount invested, leading to a linear cost function. When costs are non-linear, the population can sometimes become dimorphic in the vicinity of a singular strategy. In this case, the two evolutionary branches diverge and may eventually end up on opposite sides of the convergence stable solution in a process is known as evolutionary branching (Geritz et al. 1997). In this case, the branches may end on opposite sides of the evolutionary repellor caused by the synergistic part of the benefit curve as well. Figure 3 A-C demonstrates (assuming no assortment) that not only is coexistence possible when the benefits are synergistic, but the coexisting community can emerge from an initially monomorphic community in small evolutionary steps. Figure 3B and 3C show the evolutionary dynamics with group size fixed ($N = 30$). If the population starts with a trait value below approximately $x = 0.2$, evolution proceeds toward zero investment. If, instead, the trait value is initially above this threshold, evolutionary branching occurs and a stable coexistence between full producers and nonproducers is eventually achieved.

Figure 3D, which depicts population dynamics between two strategies, shows that the coexistence is maintained by frequency-dependent population dynamics. If, however, a high enough frequency of nonproducers would for any reason accumulate in the population, the producers will be eliminated leaving only nonproducers. We have a wide range of outcomes for a single benefit and cost function: full investment by all; full investment by some proportion of the population and zero investment by all others; and zero investment by all – dependent only on initial conditions and group size. In this example, all singular strategies are evolutionarily unstable, but as equation 3 shows, group size can also determine whether a population evolves toward an intermediate evolutionarily stable investment level or whether a dimorphic population emerges.

We have until now assumed random assortment among all individuals in the population ($\rho = 0$). This may be acceptable in situations where the individuals are interpreted as founders which may have dispersed from afar, but in many other biological contexts, the groups will not be well-mixed. As shown in figure 4, high assortment makes cooperation more likely to evolve; compared to plots in figure 2 in the bifurcation plots of singular strategies, the repelling branches (convergence unstable) are lowered and the attracting (convergence stable) branches are raised. This is because the benefits grow but there is no longer the need to split the spoils among many genotypes. This relates to previous work with discrete types demonstrating that assortment decreases the critical cost for a mixed equilibrium between cooperators and defectors Archetti 2009a,b. Assortment is especially important in large groups where direct benefits are not alone sufficient to maintain cooperation. Sufficiently high relatedness values may allow cooperation to be maintained at some positive level for arbitrarily high group sizes, even when the benefit function is diminishing or sigmoidal (in contrast to fig. 2). From equation 4, with linear costs, cooperation is stable at arbitrarily high group sizes when the maximum value of $B'(x)$ exceeds c/r_w (see Online Appendix). If cooperation is convergence stable at some group size with no assortment ($r_o = 0$), then in a clonal population ($r_o = 1$) a positive level of cooperation is also convergence stable at arbitrarily high group sizes. Equations 5 and 6 make clear that the conditions for evolutionary branching are very dependent on both the mean and variance of ρ. We give an example in the Online Appendix where changing $\mathrm{Var}(\rho)$ can alter evolutionary stability without affecting convergence stability, thus determining whether evolutionary branching occurs.

In figure 5, we show the joint evolution of the trait for public goods production and the quorum sensing threshold group size above which the trait is expressed (see equation 7). In this case, costs and benefits of expression correspond to those in figure 2C. At each generation, a group is formed of size 5 or size 45 with equal probability. When the public good is constitutively produced, the population always ends at nonproduction, then unstable even at large group sizes. In contrast when group size dependent regulation of the trait is allowed to evolve, the cooperation can be maintained. The threshold (s) can evolve such that the cooperative trait is not expressed at the low group size (5) but is expressed at other group sizes, when it is advantageous (see Online Appendix for an example). Figure 5 also reveals that when the investment value x is sufficiently low, the threshold s is expected to increase which can make investment less likely to subsequently increase.

Discussion

Our results underline several important caveats for experiments on microbes. In pairwise invasibility experiments, it is important to realize that just because a producer may be unable to invade cheats when at low frequencies, this does not necessarily mean it cannot be very stably maintained at higher frequencies. So even if cheats invade cooperators but not the reverse, coexistence at intermediate levels may still be possible. After the demonstration that a producer is exploited by a cheat one should also test how producers fare at different starting frequencies. It is possible above some starting frequencies, producers will achieve intermediate abundances, but below this threshold will be lost.

Our analysis also points to the potential complexities of varying density in microbe experiments. If laboratory results using well-mixed cultures do not accord with natural settings, differences in density in addition to relatedness should be explored. For instance, figures 3 and 4 show that density in addition to relatedness can be crucial to the qualitative evolutionary dynamics. In figure 4, in the simplest case with no assortment, group size and initial conditions determine whether all nonproducers, all cheats, or some combination of the two will be reached; as equation 3 shows, group size can also determine whether a uniform level of intermediate investment is the evolutionary endpoint or whether the population splits into a dimorphism. Microbe experiments are characterized by bacterial populations in high densities in nutrient-rich and enemy-free environments, which can be vastly different from many natural environments, and these differences must be carefully considered.

In this paper we have focused primarily on the shapes of benefit functions in social evolution, and a significant part of our consideration was the repellor that can arise from sigmoidal functions. When we considered nonlinear cost functions, it was only to understand their effect on evolutionary branching. However, diminishing cost functions in addition to synergy can possibly lead to evolutionary repellors (see Online Appendix A1). Additionally, evolutionary repellors exist in other, noncooperative contexts as well. For instance, dynamics qualitatively similar to the sigmoidal case have been demonstrated in epidemiological contexts, dependent on tradeoffs in parasite transmission strategies (Ferdy and Godelle 2005).

Whenever synergy exists, the benefit curve will most likely be sigmoidal, since benefits cannot accelerate indefinitely. The most significant qualitative difference between the diminishing functions that are typically assumed and sigmoidal functions is that the latter often permits an evolutionary repellor, making non-production locally stable (figure 2C). Once above this repellor, public goods production is stable, and we have shown that gradual evolution in addition to loss of function mutations can lead to a coexistence between producer and nonproducer. But how does the population cross the repellor initially from below, allowing cooperation to be established? Kin selection theory offers one explanation. As figure 3 shows, in assorted populations for high group sizes, the repellor becomes arbitrarily close to zero, lowering the hurdle to production. With sufficiently high relatedness, cells in high densities do not need to share the spoils among many genotypes, and thus cooperation can be maintained at arbitrarily high densities. This assortment, along with a jump in phenotype space by mutation or acquisition of mobile genetic elements may allow this repellor to be overcome (Smith 2001; Nogueira et al. 2009; Rankin et al. 2011). Even after this crossover, the evolutionary trap is always present, and if long enough spans of time are spent in low density populations as is common in many bacteria at some point in their lifecycles, the cooperative trait value can drop below the repellor and be lost forever.

One mechanism to avoid the evolutionary trap created by synergy is density-dependent gene regulation or quorum sensing. The evolutionary advantage of quorum sensing is usually phrased as limiting expression of particular genes to certain cellular densities. Cells which express genes only at high densities, when they receive a benefit, gain a fitness advantage over a nonregulated counterpart. We have shown that quorum sensing can prevent non-producers from invading when density is too low, limiting the cheat load that could otherwise sink cooperation. The density-dependent increase in fitness may be nonsynergistic (Brookfield 1998; Brown and Johnstone 2001; Czárán and Hoekstra 2009) due to, for instance, reduced loss of secretions into the environment at high cellular densities. In contrast, figure 5 shows that when the regulated trait is synergistic, this effect can prevent the trait from falling below the evolutionary repellor. In either scenario, quorum sensing may help maintain public goods production in the population by upregulating it only when favored by natural selection. However in the synergistic case, quorum sensing also helps prevent the collapse of cooperation while cells grow in low-density environments (figure 5).

Many bacteria spend much of their time in low densities until their environment changes upon, for example, entering a host. By restricting expression to high density, cooperation is not diminished when at low numbers for relatively long periods of time. Though low densities can cause declines in production regardless of the cause of group augmentation, in the synergistic cases (2B and 2C), the situation is especially dire. Restricting expression to high population sizes effectively bypasses the synergistic portion of the benefit function, and consequently, the cooperative trap (below which cooperation may not recover) is avoided (figure 5). There are several adaptive explanations for autoinduction sensing, including to sense density, to sense diffusion properties, and even to sense the presence of other strains of bacteria (Brookfield 1998; Redfield 2002). Whatever this mix of adaptive functions selecting for quorum sensing, the prevention of widespread cooperative collapse may be an important consequence. However, we also see in figure 5 that quorum sensing does little to help cooperation initially overcome the repellor. In fact, at very low levels of production (under the evolutionary repellor), the quorum sensing threshold may actually increase and make stable cooperation even more difficult to achieve. So quorum sensing is unhelpful in crossing the repellor initially but may be crucial for the maintenance of cooperation by preventing a population from slipping into the trap after cooperation has already been established.

It would be interesting to integrate our work into a more demographically sophisticated model. As a result of groups being reformed at each generation in our model, successful individuals replace other individuals drawn from the entire population, rather than more realistic models with limited dispersal in viscous populations (Wright 1949; Hamilton and May 1977; Rousset 2004). This limited dispersal causes competition among patchmates which can have major effects on evolution (Hamilton and May 1977; Taylor 1992). Equation 6 indicates that higher variance of the degree of assortment among groups in a population can make the conditions for evolutionary branching more narrow; this would be interesting to study further in the context of the effects on evolutionary branching of various dispersal regimes (Ajar 2003). Another possible consideration for future work is that in our model, the individual traits did not affect relatedness. However a feedback between the trait and relatedness is possible, as in the classic example of the evolution of dispersal rates (Hamilton and May 1977; Rousset and Ronce 2004) where dispersal rate affects relatedness and vice versa (Lion and van Baalen 2008; Lehmann and Rousset 2010). This could also occur when the patch size increases with public goods production; if a patch has a higher carrying capacity dependent on cooperation within it, synergistic functions may lead to interesting dynamics.

To experimentally test this model one must first determine the cost and benefit curve for production of a public good. The benefit can be deduced using a knockout strain supplemented with various quantities of the public good, and the cost can be determined from growth in a strain with an inducible promoter for the public good in an environment where the public good does not give additional growth advantage (e.g. when iron is not limiting if siderophore production is the trait of interest). From this, basic predictions can be made about the dynamics of the system as in figures 2 and 4. A first approximation is possible by altering bacterial densities with differing fractions of wildtype and knockout strains (figure 3D), however this ecological experiment neglects the cost function entirely; if the cost function is approximately linear up to the wildtype levels however one can understand the basic dynamics. More directly, predictions can be tested experimentally by following the evolutionary trajectory of constitutive strains with differing starting production levels (potentially engineered by a set of mutations on the genes responsible for the trait) at different densities.

We should reiterate that a particular microbe may best be represented by different functional forms from what we use here. For instance, we did not consider the possibility that in high densities, fewer molecules are lost into the environment which would also increase group benefits at higher densities. In addition to this, some microbes have preferential access to their own public goods products even when in a well-mixed environment (Gore et al. 2009). For example, we could allow producers to get a benefit greater than the equal share of production we give them in the model studied here. However, even in microbes with properties different than those specified here, synergy will likely play a prominent role. Lastly, the interplay between the production and regulation in our model made simplifying assumptions about the evolution of autoinduction thresholds, and in reality a particular quorum sensing network can regulate many traits, rather than only one. With many traits, the quorum sensing trait will be likely be more stable. The evolvability of various features of quorum sensing (in this case, the group size at which autoinduction occurs) has not received significant attention in the literature, however there is evidence that various aspects of the quorum sensing are evolveable (Ansaldi and Dubnau 2004; Ichihara et al. 2006; Sandoz et al. 2007). Future work integrating molecular details into the evolution of these thresholds could be very interesting.

Online Appendix

A1. Derivation of selection gradient and stability with genetic assortment

At each generation, an individual is identical by descent to some number in its group including itself (among the total group members N), which is a random variable K. We define Pr(k) as the probability that a rare mutant in the population has exactly $k-1$ other genetically identical mutants in its group. Thus, $\langle K \rangle = \sum_{k=1}^{N} k\mathrm{Pr}(k)$ is the expectation of the number of mutants in a random mutant's group, and $\langle K \rangle / N$ is the likelihood that a recipient of the mutant's act is also a mutant, again assuming mutants are rare in the population. So with no assortment $\mathrm{Pr}(1) = 1$, and with assortment $\mathrm{Pr}(1) < 1$. Our expression for relatedness of a rare mutant to a random individual in its group is just the expected genotype of a recipient's genotype to that of the actor (unity) (Grafen 1985) which is:

$$r_w = \frac{\langle K \rangle}{N} = \sum_{k=1}^{N} \frac{k}{N} \mathrm{Pr}(k). \tag{A1}$$

This is whole-group relatedness (r_w) which is of interest since cooperators get a direct benefit from their own cooperation. (Others-only relatedness, or r_o, is relatedness to recipients other than the focal cooperator itself with $r_w = r_o \frac{N-1}{N} + \frac{1}{N}$ (Pepper 2000). This value is the same as $\langle \rho \rangle$ in the main text). The expected payoff of an individual with trait y in a monomorphic population with trait value x is given by

$$P(y,x) = \sum_{k=1}^{N} \frac{\mathrm{Pr}(k) B(ky + (N-k)x)}{N} - C(y). \tag{A2}$$

From this, the selection gradient becomes:

$$D(x) = \sum_{k=1}^{N} \frac{k\Pr(k)B'(Nx)}{N} - C'(x) \tag{A3}$$

$$= r_w B'(Nx) - C'(x) = \frac{B'(Nx)(1 + r_o(N-1))}{N} - C'(x), \tag{A4}$$

The solutions of $D(x^*) = 0$ are the singular strategies. The condition for convergence stability of a singular strategy is:

$$\frac{\partial D}{\partial x}|_{x=x^*} = NB''(Nx^*)r_w - C''(x^*) \tag{A5}$$

$$= B''(Nx^*)(1 + r_o(N-1)) - C''(x^*) < 0, \tag{A6}$$

Using ρ from the main text, this condition is simply:

$$\frac{\partial D}{\partial x}|_{x=x^*} = NB''(Nx^*)r_w - C''(x^*) \tag{A7}$$

$$= B''(Nx^*)(1 + \langle\rho\rangle(N-1)) - C''(x^*) < 0, \tag{A8}$$

and for evolutionary stability:

$$\frac{\partial^2 P}{\partial y^2}|_{y=x^*} = \frac{1}{N}\sum_{k=1}^{N} \Pr(k)k^2 B''(Nx^*) - C''(x^*) \tag{A9}$$

$$= \frac{B''(Nx^*)}{N}\sum_{k=1}^{N} \Pr(k)k^2 - C''(x^*) < 0. \tag{A10}$$

Now

$$\mathrm{Var}(K) = \sum_{k=1}^{N} \Pr(k)(k - \langle K\rangle)^2 \tag{A11}$$

$$\sum_{k=1}^{N} \Pr(k)k^2 = 2\sum_{k=1}^{N} \Pr(k)k\langle K\rangle - \sum_{k=1}^{N} \Pr(k)\langle K\rangle^2 + \mathrm{Var}(K) \tag{A12}$$

$$\sum_{k=1}^{N} \Pr(k)k^2 = \langle K \rangle^2 + \mathrm{Var}(K) \tag{A13}$$

By using ρ from the main text, the condition for evolutionary stability becomes:

$$\frac{B''(Nx^*)}{N}[(1+(N-1)\langle\rho\rangle)^2 + \mathrm{Var}(\rho)(N-1)^2] - C''(x^*) < 0. \tag{A14}$$

A2. Assuming linear costs and nondecreasing benefits, if a positive level of cooperation evolves without assortment at some group size N0, then a positive level of cooperation evolves in arbitrarily large group sizes when $r_o > 1/N_0$:

For some x_o, N_0,the selection gradient is positive:

$$\frac{B'(N_0x_0)}{N_0} - c > 0. \tag{A15}$$

Now for some arbitrarily high N_1, let $x_1 = \frac{N_0x_0}{N_1}$. The selection gradient now is

$$\frac{B'(N_1x_1)}{N_1} + \frac{r_o(N_1-1)B'(N_1x_1)}{N_1} - c > 0. \tag{A16}$$

which is equivalent to

$$r_oB'(N_1x_1) + \frac{B'(N_1x_1)(1-r_o)}{N_1} - c \tag{A17}$$

Now, so long as $r_o > 1/N_o$, this gradient is positive since the first term itself is greater than c.

A3. Variance can affect evolutionary branching

Here we show an example (fig A3) of a situation where $\langle \rho \rangle$ is constant but $\mathrm{Var}(\rho)$ is not, and this distinction determines whether evolutionary branching occurs. When $N = 4$, variance may be zero if every group has two individuals of one genotype and two of another, or it may follow a binomial distribution with $\langle \rho \rangle = 1/3$. Both of these give $\langle\ r_w \rangle = 1/2$.

A4. Quorum sensing model

The payoff to an individual with trait values x and s in two distinct group sizes N_1 and N_2 is:

$$P_1 = \frac{B\left(Q(s_1, N_1)x_1 + \ldots + Q(s_{N_1}, N_1)x_{N_1}\right)}{N_1} - C\left(Q(s_i, N_1)x_i\right) \tag{A18}$$

$$P_2 = \frac{B\left(Q(s_2, N_2)x_2 + \ldots + Q(s_{N_2}, N_2)x_{N_2}\right)}{N_2} - C\left(Q(s_i, N_2)x_i\right) \tag{A19}$$

where $Q(s_i, N) = 1/(1 + e^{s_i - N})$ as in the main text. The expected payoff then for a pair (x, s), given that the individual randomly joins one of the two group sizes is $P = (P_1 + P_2)/2$. The singular strategies occur when $\frac{\partial P}{\partial x} = \frac{\partial P}{\partial s} = 0$, and these zeros of these selection gradients define the isoclines of figure 5. See (Geritz et al. 1997; Brown and Taylor 2010) for details of analyzing systems of multiple trait evolution.

References

É. Ajar. Analysis of disruptive selection in subdivided populations. *BMC Evolutionary Biology*, 3(1):22, 2003.

M. Ansaldi and D. Dubnau. Diversifying selection at the bacillus quorum-sensing locus and determinants of modification specificity during synthesis of the comx pheromone. *Journal of bacteriology*, 186(1):15, 2004.

M Archetti. Cooperation as a volunteer's dilemma and the strategy of conflict in public goods games. *Journal of Evolutionary Biology*, 22(11):2192–2200, 2009a. ISSN 1420-9101.

Marco Archetti. The volunteer's dilemma and the optimal size of a social group. *Journal of Theoretical Biology*, 261(3):475–480, 2009b. ISSN 1095-8541.

Å. Brännström and U. Dieckmann. Evolutionary dynamics of altruism and cheating among social amoebas. *Proceedings: Biological Sciences*, 272:1609–1616, 2005.

Å. Brännström, T. Gross, B. Blasius, and U. Dieckmann. Consequences of fluctuating group size for the evolution of cooperation. *J Math Biol*, 2010.

J. F. Y Brookfield. Quorum sensing and group selection. *Evolution*, 52:1263–1269, 1998.

S. P. Brown and R. A. Johnstone. Cooperation in the dark: Signalling and collective action in quorum-sensing bacteria. *Proceedings: Biological Sciences*, 268:961–965, 2001.

S. P. Brown, S. A. West, S. P. Diggle, and A. S. Griffin. Social evolution in micro-organisms and a trojan horse approach to medical intervention strategies. *Philosophical Transactions of the Royal Society B*, 364:3157–3168, 2009.

S.P. Brown and R. Kümmerli. Molecular and regulatory properties of a public good shape the evolution of cooperation. *Proceedings of the National Academy of Sciences*, 2010.

S.P Brown and P.D. Taylor. Joint evolution of multiple social traits - an inclusive fitness analysis. *Proceedings of the Royal Society of London B*, 277:415–422, 2010.

J.S. Chuang, O. Rivoire, and S. Leibler. Cooperation and hamilton's rule in a simple synthetic microbial system. *Molecular systems biology*, 6(1), 2010.

T. Clutton-Brock. Breeding together: kin selection and mutualism in cooperative vertebrates. *Science*, 296(5565):69, 2002.

T. Czárán and R. F. Hoekstra. Microbial communication, cooperation and cheating: Quorum sensing drives the evolution of cooperation in bacteria. *PLoS ONE*, 4:1–10, 2009.

Kuiying Deng and Tianguang Chu. Adaptive evolution of cooperation through darwinian dynamics in public goods games. *PLoS ONE*, 6(10):e25496, 2011.

U. Dieckmann and R. Law. The dynamical theory of coevolution: a derivation from stochastic ecological processes. *Journal of Mathematical Biology*, 34(5):579–612, 1996.

S. P. Diggle, A. S. Griffin, G. S. Campbell, and S. A. West. Cooperation and conflict in quorum-sensing bacterial populations. *Nature*, 450:411–414, 2007.

M. Doebeli, C. Hauert, and T. Killingback. The evolutionary origin of cooperators and defectors. *Science*, 306:859–862, 2004.

J.B. Ferdy and B. Godelle. Diversification of transmission modes and the evolution of mutualism. *The American Naturalist*, 166(5):613–627, 2005.

K. R. Foster. Diminishing returns in social evolution: the not-so-tragic commons. *Journal of Evolutionary Biology*, 17:1058–1072, 2004.

W. C. Fuqua, S. C. Winans, and P. E. Greenberg. Census and consensus in bacterial ecosystems: the luxr-luxi family of cell quorum-sensing regulators. *Annual Review of Micriobiology*, 50:727–751, 1996.

A. Gardner, S. A. West, and A. Buckling. Bacteriocins, spite and virulence. *Proceedings of the Royal Society of London B*, pages 1529–1535, 2004.

S. A. H. Geritz, E. Kisdi, G. Meszeˊna, and J. A. J. Metz. Evolutionarily singular strategies and the adaptive growth and branching of the evolutionary tree. *Evolutionary Ecology*, 12 (1):35–57, 1997. ISSN 0269-7653.

J. Gore, H. Youk, and A. Oudenaarden. Snowdrift game dynamics and facultative cheatingin yeast. *Nature*, 459:253–256, 2009.

A. Grafen. A geometric view of relatedness. *Oxford Surveys in Evolutionary Biology*, 2: 28–90, 1985.

A. S. Griffin, S. A. West, and A. Buckling. Cooperation and competition in pathogenic bacteria. *Nature*, 430:1024–1027, 2004.

W.D. Hamilton and R.M. May. Dispersal in stable habitats. *Nature*, 1977.

A. V. Hill. The possible effects of the aggregation of the molecules of haemoglobin on its dissociation curves. *J Physiol*, 40(4), 1910.

H. Ichihara, K. Kuma, and H. Toh. Positive selection in the comc-comd system of streptococcal species. *Journal of bacteriology*, 188(17):6429, 2006.

L. Keller. *Levels of Selection in Evolution*. Princeton University Press, 1999.

H. Kokko, R. A. Johnstone, and T. H. Clutton-Brock. The evolution of cooperative breeding through group augmentation. *Proceedings of the Royal Society of London B*, pages 187–196, 2000.

L. Lehmann and F. Rousset. How life history and demography promote or inhibit the evolution of helping behaviours. *Philosophical Transactions of the Royal Society B: Biological Sciences*, 365(1553):2599, 2010.

Sebastien Lion and Minus van Baalen. Self-structuring in spatial evolutionary ecology. *Ecology Letters*, 11(3):277–295, 2008.

R.C. MacLean and I. Gudelj. Resource competition and social conflict in experimental populations of yeast. *Nature*, 441(7092):498–501, 2006. ISSN 0028-0836.

T. Nogueira, D.J. Rankin, M. Touchon, F. Taddei, S.P. Brown, and E.P.C. Rocha. Horizontal gene transfer of the secretome drives the evolution of bacterial cooperation and virulence. *Current Biology*, 19(20):1683–1691, 2009. ISSN 0960-9822.

J. W. Pepper. Relatedness in trait group models of social evolution. *Journal of Theoretical Biology*, pages 355–368, 2000.

D.C. Queller. Kinship, reciprocity and synergism in the evolution of social behaviour. *Nature*, 318(6044):366–367, 1985. ISSN 0028-0836.

D.J. Rankin, E.P.C. Rocha, and S.P. Brown. What traits are carried on mobile genetic elements, and why? *Heredity*, 106:1–10, 2011.

R.J. Redfield. Is quorum sensing a side effect of diffusion sensing? *TRENDS in Microbiology*, 10(8):365–370, 2002. ISSN 0966-842X.

N. D. Robson, A. R. J. Cox, S. J. McGowan, B. W. Bycroft, and G. P. C. Salmond. Bacterial n-homoserine-lactone-dependent signalling and its potential biotechnological applications. *Trends in Biotechnology*, 15:258–264, 1997.

A. Ross-Gillespie, A. Gardner, A. Buckling, S. A. West, and A. S. Griffin. Density dependence and cooperation: Theory and a test with bacteria. *Evolution*, 63:2315–2325, 2009.

F. Rousset. *Genetic structure and selection in subdivided populations*. The Princeton University Press, 2004.

F. Rousset and O. Ronce. Inclusive fitness for traits affecting metapopulation demography. *Theoretical population biology*, 65(2):127–141, 2004.

K.M. Sandoz, S.M. Mitzimberg, and M. Schuster. Social cheating in pseudomonas aeruginosa quorum sensing. *Proceedings of the National Academy of Sciences*, 104(40):15876, 2007.

J. Smith. The social evolution of bacterial pathogenesis. *Proceedings of the Royal Society of London. Series B: Biological Sciences*, 268(1462):61, 2001. ISSN 0962-8452.

J. Smith, J.D. Van Dyken, and P.C. Zee. A generalization of hamilton's rule for the evolution of microbial cooperation. *Science (New York, NY)*, 328(5986):1700, 2010.

J. Maynard Smith and E. Szathmáry. *The Major Trnasitions in Evolution*. Oxford University Press, 1995.

D. J. T. Sumpter. *Collective Animal Behavior*. Princeton University Press, 2010.

D. J. T. Sumpter and Åke Brännström. *Synergy in Social Communication*. Oxford University Press, 2008.

P.D. Taylor. Inclusive fitness in a homogeneous environment. *Proceedings of the Royal Society of London. Series B: Biological Sciences*, 249(1326):299–302, 1992.

S. A. West, A. S. Griffin, A. Gardner, and S. P. Diggle. Social evolution theory for microorganisms. *Nature*, 4:597–604, 2006.

S.A. West and A. Buckling. Cooperation, virulence and siderophore production in bacterial parasites. *Proceedings of the Royal Society of London. Series B: Biological Sciences*, 270 (1510):37, 2003.

P. Williams, M. Camara, A. Hardman, S. Swift, D. Milton, V.J. Hope, K. Winzer, B. Middleton, D.I. Pritchard, and B.W. Bycroft. Quorum sensing and the population-dependent control of virulence. *Philosophical Transactions of the Royal Society of London. Series B: Biological Sciences*, 355(1397):667, 2000.

S. Wright. The genetical structure of populations. *Annals of Human Genetics*, 15(1):323–354, 1949.

FIGURE CAPTIONS

fig 1: Accelerating, decelerating, and sigmoidal benefit functions. A) Total benefit as a function of total public goods investment Nx, expressed as the product of the group size N and the cooperative investment per individual, x. The solid and dashed lines represent synergistic (accelerating) benefits as they have positive concavity for some intervals, whereas the dotted line always represents diminishing returns. B) Corresponding per-capita benefit $B(Nx)/N$ as a function of group size, N, assuming that every individual cooperates at some fixed amount (here, $x = 1$, meaning full cooperation). The benefit functions used are $B(x) = \alpha(\beta + de^{\kappa - bx})^{-1} - \alpha(\beta + de^{\kappa})^{-1}$ with $\alpha = 10^5$, $d = 1$, $\beta = 1$, $\kappa = 0$, and $b = 0.1$ (decelerating benefits; dotted line), $B(x) = bx^a$ with $b = 0.1$ and $\alpha = 3$ (accelerating benefits; dashed line), and $\alpha(\beta + de^{\kappa - bx})^{-1} - \alpha(\beta + de^{\kappa})^{-1}$ where $\alpha = 90000$, $d = 1$, $\beta = 2$, $\kappa = 10$, $b = 0.2$. (sigmoidal benefits; solid line).

fig 2: Bifurcation plots illustrating the evolutionary dynamics with decelerating, accelerating, and sigmoidal benefit functions. The solid lines indicate the location of interior singular strategies for different group size N. Arrows indicate the direction of gradual evolution of a monomorphic population. A) Decelerating benefits. There is a unique evolutionarily stable strategy which decreases with group size. When group sizes are greater than approximately 80, cooperation is entirely disfavored. ($B(x) = \alpha(\beta + de^{\kappa - bx})^{-1} - \alpha(\beta + de^{\kappa})^{-1}$ with $\alpha = 2000$, $d = 1$, $\beta = 1$, $\kappa = 0$, and $b = 0.8$) B) Accelerating benefits. For small group sizes there is a unique evolutionarily stable strategy corresponding to full defection. As the group size increases, full cooperation also becomes an evolutionarily stable strategy. Any interior singular strategy is repelling and decreases with group size, but never reaches zero. ($B(x) = bx^a$

with $b = 0.1$ and $\alpha = 3$) C) Sigmoidal benefits. Up to two interior singular strategies are possible, one repelling and the other attracting. ($B(x) = \alpha(\beta + de^{\kappa - bx})^{-1} - \alpha(\beta + de^{\kappa})^{-1}$ where $\alpha = 10000$, $d = 1$, $\beta = 2$, $\kappa = 7$, and $b = 0.3$). Each convergent stable attractor could potentially be an evolutionary branching point. The cost function used is $C(x) = cx$ with $c = 5$.

fig 3: Evolutionary branching and the emergence of two coexisting strategies of full defection and full cooperation in a setting with sigmoidal benefits and non-linear costs. A) Bifurcation plot illustrating the effects of group size on directional selection for the function used in the other diagrams in the figure. B) A pairwise invasibility plot (PIP) illustrating the monomorphic evolutionary dynamics. There are two singular strategies at approximately $x = 0.2$ and $x = 0.4$ of which only the latter is convergence stable. Monomorphic populations with trait values above the first singular strategy will evolve towards the second singular to the singular strategy where they undergo disruptive selection and subsequently evolutionary branching. C) Individual-based simulation demonstrating evolutionary branching at approximately $x = 0.4$, thus corroborating the predictions from the PIP. The inserted panel shows the evolutionary dynamics for populations which initially have trait values lower than the first singular strategy at approximately $x = 0.2$; here investment decreases to zero. D) Population dynamics of the resultant coexisting strategies of full defection ($x = 0$) and full cooperation ($x = 1$). If the fraction of cooperators is initially below approximately 18%, the cooperators will be eliminated altogether. Otherwise, the population dynamics will result in a stable coexistence with approximately 45% cooperators. The sigmoidal benefit function used is the same as in figure 1, $B(x) = b(x^3 + \beta x^2)(x^2 + \alpha)^{-1}$, but with different parameters $b = 200$,

$\beta = 450$, $\alpha = 180$. The non-linear cost function used is $C(x) = c_1 x - c_2 x^2$ with $c_1 = 170$, $c_2 = 50$. The assumed group size in B-D is $N = 30$.

fig 4: Effect of assortment (positive relatedness) on the evolutionary dynamics of decelerating, accelerating, and sigmoidal benefit functions. Displayed are different degrees of others-only relatedness (which are equal to the values of $\langle\rho\rangle$): $r_o = 0$, $r_o = 0.01$, and $r_o = 0.5$. Solid lines indicate attracting (convergence-stable) singular strategies, while dashed lines indicate singular strategies which are repelling (not convergence stable). Panels A, B, and C have use all the same benefit and cost functions as in figure 2.

fig 5: Joint evolution of the public goods production trait x and the group-size threshold s, above which the production is expressed. Benefits and costs are as in figure 2C. At each generation, a group is formed of size 5 or size 45 with equal probability. For very low quorum sensing thresholds, production is not affected by changes in group size and evolution inevitably brings the production down to zero. However, for an intermediate range of the quorum sensing threshold s, public goods production can be stably maintained. This is true even if the threshold and production is allowed to co-evolve, provided that initial state is a population with an intermediate quorum sensing threshold and a sufficiently high production. For other initial conditions, co-evolution will bring the production down to zero and increase the threshold to arbitrarily large values.

fig A1: The effect of variance on evolutionary branching when whole-group relatedness $r_w = 1/2$. A) The blue line is the singular strategy which is convergent stable. The two other curves enclose the area for evolutionary stability of the binomial (magenta) and fixed (tan) cases. B) Simulation with $N = 4$ in the binomial case. C) Simulation with $N = 4$ in the fixed case. (For all panels, $B(x) = \alpha(\beta + de^{\kappa - bx})^{-1} - \alpha(\beta + de^{\kappa})^{-1}$ where $\alpha = 800$, $d = 1$, $\beta = 1$, $\kappa = 0$, and $b = 1.3$. $C(x) = c_1 x - c_2 x^2$ with $c_1 = 130$ and $c_2 = 50$.)

fig A2: The functional shape of $Q(N)$ with a threshold of $s = 10$.

fig A3: Simulation run of the joint evolution of x and s. The costs and benefits are the same as those in figure 2C of the main text. The group size is randomly chosen between $N = 5$ and $N = 45$. The quorum sensing cut-off evolves above 5, and so cooperation can be maintained.

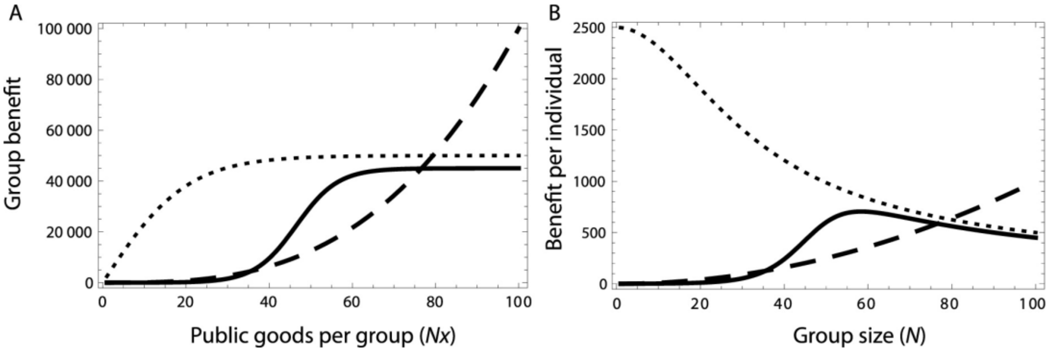

Figure 1

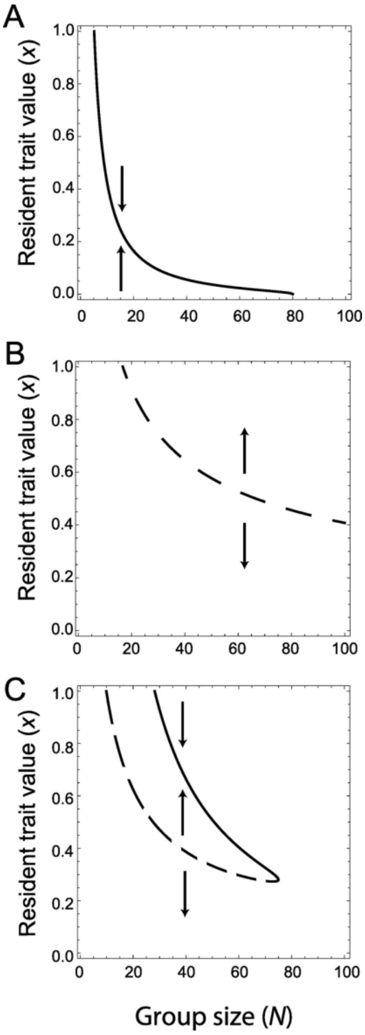

Figure 2

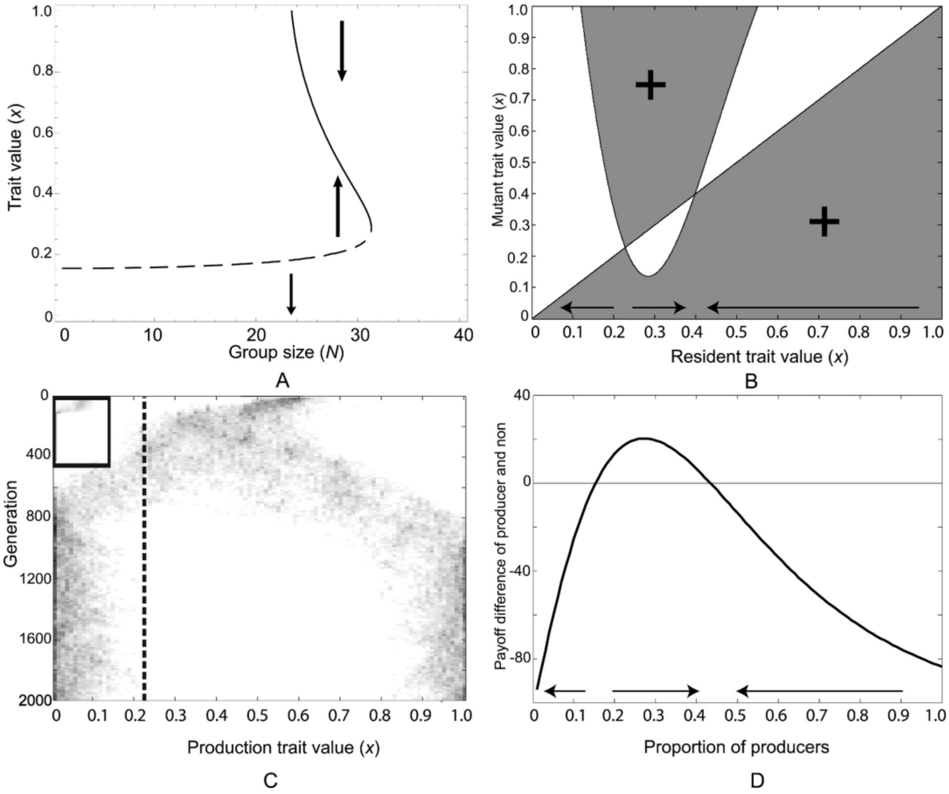

Figure 3

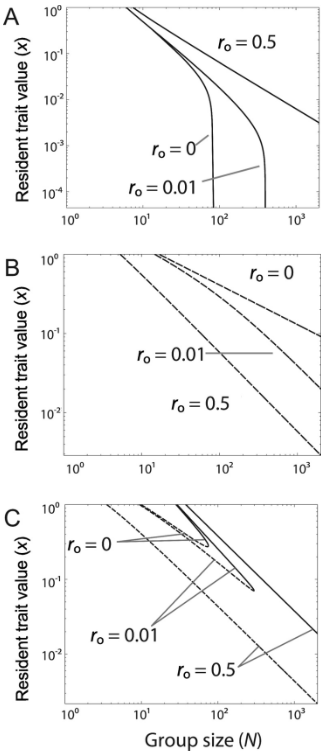

Figure 4

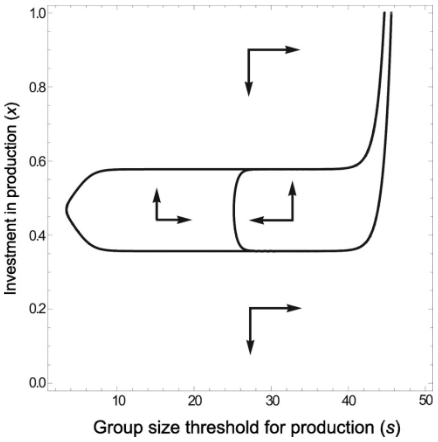

Figure 5

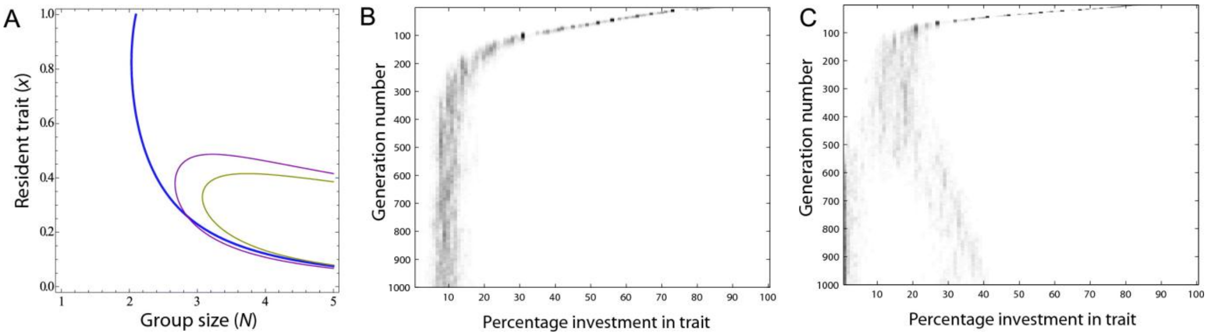

Figure A1

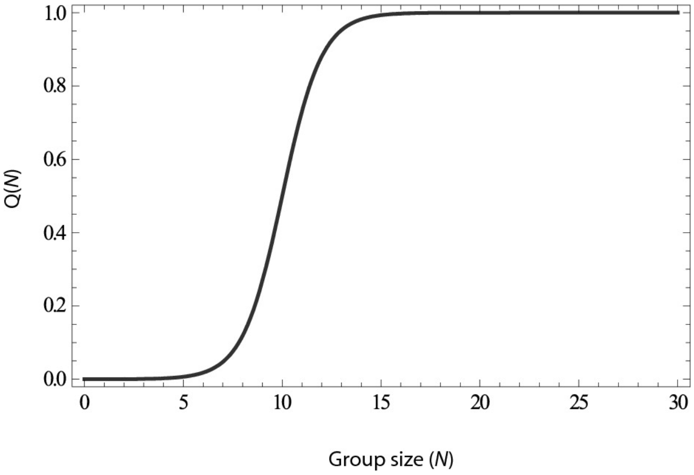

Figure A2

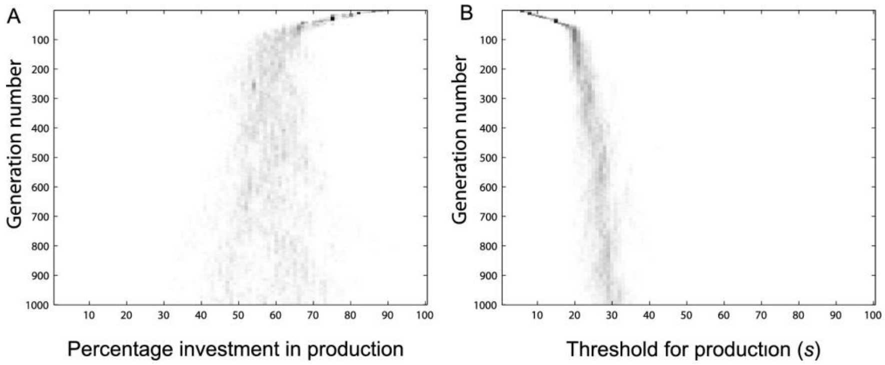
A
B
Generation number
100
200
300
400
500
600
700
800
900
1000
10
20
30
40
50
60
70
80
90
100
Percentage investment in production
Threshold for production (s)

Figure A3

Chapter 2: Shared toxins cause the failure of the Independent Action Hypothesis in a bacterial pathogen

Introduction:

In even the best-studied host-pathogen systems, the exact relation between the number of consumed cells and probability of infection, or the dose-response, is unclear. This relationship is not only of basic scientific interest (Zwart et al., 2011, 2009) but is also important to accurately gauge infection risk in exposed communities (Artiola et al., 2004; Buchanan et al., 2009; Canter, 2005; Cox, 2006; Fazil, 2005; Haas et al., 1999; *Hazard Characterization for Pathogens in Food and Water*, 2004; National Research Council, 2005; Westcot, 1997). Unfortunately, the doses of bacteria that are of greatest public health relevance are usually so low that they are difficult to experimentally investigate in most systems. Even when measuring out a precise number of infecting particles is possible, the signal-to-noise ratio is so low at these doses that most experiments lack statistical power. To address this, experimental data taken at high doses are extrapolated to low doses using one of several mathematical models that approximate the dose-response relationship. These models are common in that they all make one basic biological assumption; they all accept the "independent action hypothesis."

The independent action hypothesis has two components. It states 1) that infecting bacteria act independently and 2) that the mean probability of initiating a fatal infection per inoculated bacterium is invariant of dose (see figure 1) (Druett, 1952; Meynell, 1957). The first of these claims is suspect in light of the fast-growing list of known social behaviours in bacteria (West et al., 2006). The second, on which standard dose-response models are built, is still largely accepted (Artiola et al., 2004; Buchanan et al., 2009; Fazil, 2005; Haas et al., 1999; Rubin, 1987; Westcot, 1997), and many epidemiological models implicitly assume it (see (Ben-Ami et al., 2008; Regoes et al., 2003)). Discussion on the independent action hypothesis (IAH) has typically centred on indirect inference. This is either based on statistical analysis of dose-response data (Ridout et al., 1993; Regoes et al., 2003; Ben-Ami et al., 2008; Fryer and McLean, 2011), or alternatively on a clever set of co-inoculation experiments (to be discussed later) measuring coinfection rates at low doses (Meynell, 1957; Moxon and Murphy, 1978; Rubin, 1987; Zwart et al., 2009). Though this work has been generally consistent with the IAH, to our knowledge the independent action hypothesis has never been directly confirmed nor rejected in any bacterial system.

Here I analyse unpublished data (collected by collaborators in Ben Raymond's group [Ben Raymond and Andrew Matthews] in Royal Holloway University of London) to test the IAH with *Bacillus thuringiensis kurstaki,* a widely occurring insect pathogen (Raymond et al., 2010), in larvae of the diamondback moth, *Plutella xylostella*. During sporulation each bacterium produces a proteinaceous toxin crystal (Cry toxin). When a group of bacteria is ingested, these crystals are solubilised in the midgut and perforate it, facilitating septicaemic proliferation in the haemolymph (Schnepf et al., 1998). These toxin crystals are "public goods" because any cell's toxins benefit all the cells in the inoculum (Raymond et al., 2012). By independently manipulating toxin dose and bacterial density, we are able to demonstrate that toxins are a limiting factor in the infection process. With insufficient total toxins, infection does not occur regardless of inoculum size. On the other hand with sufficiently high toxin levels, inoculum size itself has very little effect on mortality. This suggests that the dominant force in shaping the dose-response is success in perforating the insect midgut, a collective process. The release of shared toxins violates the first claim of the IAH, and likely causes the second claim to fail as well. By using data from independent manipulations of spores and toxin crystals, I argue that there is reason to question the possibility of independently fitting a probability of infection to each infecting bacteria, however this case is not yet definitive. Then I analyse dose response curves from wildtype *B.t.* spores. I fit the dose-response data to the two most popular dose-response models, the exponential and the beta-exponential curves. The exponential model (assuming homogeneity in host susceptibility) greatly underestimates risk at the low doses. The beta-exponential model (which accounts for variability in susceptibilities) generally fits the data well but makes implausible assertions on the degree of host variability; moreover this fit significantly overestimates risks at low doses. I propose an alternative model to account for the cooperative nature of the system. I close with by arguing that formulation of dose response models should be driven by careful consideration of mechanisms of pathogenesis.

Results:

Testing the Independent Action Hypothesis in our system

Previous work indicates that that the first element of the IAH, that bacteria do not interact, is incorrect in our model system; there are indeed interactions between bacteria which is mediated by toxin secretion (Raymond et al, 2012). However it is conceivable that even with shared toxins, the second component of the IAH (that each bacterium can be assigned an independent probability of causing infection) may not be violated. Ben Raymond's group was able to experimentally separate the contribution toward mortality of Cry toxins that *B. thuringiensis* produces from the quantity of inoculated spores. They did this by using knockout mutants that did not produce the toxin and supplemented them with toxin inclusion bodies (IBs) produced by an engineered E. coli strain (see methods). They conducted two types of experiments to tease these two variables apart. They first fixed the number of spores to 900 while increasing the quantity of toxins (IBs) supplemented. In this constant spore dose experiment, increasing doses of toxin had a large impact on larval mortality (glm logistic regression slope of 0.0033, $p<0.0001$); here with fixed spore doses (fixed high at 900 spores), increasing toxins greatly increased the infection rate (figure 2).

Next there were two blocks of experiments with constant toxin doses with the number of spores varying, one supplemented with 100 toxin IBs and one with 300 (figure 3). Here the spore number had a surprisingly small effect on mortality. Spores contribute significantly to the virulence of *B. thuringiensis* infections, but this contribution is relatively minor (increasing spore dose by three orders of magnitude delivers roughly a 20% increase in mortality), with the important exception at low doses of toxin. In this case the presence of some spores, as opposed to none at all, makes a substantial contribution to mortality. Inspection of the data indicated that at low toxin concentration there was a substantial increase in mortality from zero to non-zero spores. These three experiments which separate toxins from spores, taken together, demonstrate that toxins act collectively and that the quantity of these toxins in an inoculum largely determines the probability of fatal infection.

It is well demonstrated that the first element of the IAH, that bacteria do not interact with each other, is incorrect in our model system (Raymond et al, 2012). However it is conceivable that even with shared toxins, the second component of the IAH (that each bacterium can be assigned an independent probability of causing infection) may not be violated. This could in principle occur if the following were both true: 1) toxins are entirely responsible for host death and spore doses (above zero) themselves do not affect mortality rate at low doses, and 2) the lethality of these toxins themselves follow independent action assumption, that is each toxin crystal has an independent likelihood of causing mortality. If these were both true, then each toxin crystal could be thought to have an independent likelihood of killing the host, and therefore since each bacterium is paired with a toxin crystal, an independent likelihood of causing death could be assigned to each bacterium.

The first requirement is that the toxins themselves determine lethality, and spore dose (aside from presence) does not matter. In figure 3 very high toxin doses (300 IBs) seem to kill the insects, and spore dose has extremely little impact on death. However at the lower dose of 100 IBs, this is no longer the case. Here there is a jump between infection rate with no spores and this rate with spores. There is a possibility that presence/absence of spores causes this difference and that the quantity of spores itself is immaterial (in other words, if the midgut is perforated, septicaemia is guaranteed so long as there is at least one spore). To test this one could do the same experiment with the toxin dose, except this time focused at lower doses, and including at least one point in the range between no spores and 14 (seven for instance) in order to show that spore number matters; if the points in between give lower death rates than the 14 dose, then spore dose itself matters at low doses and an independent likelihood of infection does not fit because probability of causing mortality per cell increases with spore dose. The second requirement for an independent probability of infection to be possible is that the effect of toxin dose itself follows independence assumptions. The constant spore data is given again in figure 3B, with only low doses plotted and a linear scale. In figure 3B, in one of the data blocks there is a jump in this mortality rate between the dose of 75 and 150 IBs that would be expected to be less than a two-fold difference under independence assumptions, when the actual increase is closer to 5-fold. However in the other block, which only has three data points in this region, at 75 IBs the risk of mortality is substantially higher. It seems likely that a similar phenomenon is occurring however with the jump at a lower value, but with the current data this is difficult to say. So in order to more strongly reject the possibility of assigning independent probability to mortality, one would need show that spore dose itself matters at low doses and/or that the toxins themselves do not follow independent action assumptions by doing the experiment(s) described above.

The common IAH-based dose-response models poorly predict infection rate at low doses

If the probability of a particular pathogen cell or its descendants clearing all host barriers is p, and the inoculum size is k, then the likelihood that infection occurs is $P(k) = 1 - (1-p)^k$. A second model known as the "exponential model" is more commonly used and accounts for variation in inoculum size (if only the expected ingested dose is known):

$$P(k) = 1 - e^{-pk}$$

The best exponential dose-response fit (maximum likelihood) for the wildtype data is shown in figure 4 (p=0.006226; AIC=230.9641). The exponential model is often further extended to account for variation in host susceptibility (Haas et al., 2000):

$$P(k) = 1 - {}_1F_1(\alpha, \alpha + \beta, -k) \approx 1 - \left(1 + \frac{k}{\beta}\right)^{-\alpha}$$

where α and β are parameters for the beta function describing the likelihood of infection of a host inoculated with one spore. The exact form is the "Hypergeometric fit" and the approximation, most accurate when $\beta > 1$ and $\alpha \ll \beta$, is known as the "Beta-Poisson". The beta-exponential model converges onto the exponential one as α approaches infinity. We plot this approximated (Beta-Poisson) version as it is used almost to the exclusion of the exact one (Hypergeometric), but this does not affect our qualitative results. The best fit for the wildtype data is also shown in figure 4 ($\alpha = 0.5374$, $\beta = 12.1732$; AIC = 32.72). Generally, beta-exponential fits are less steep than exponential because when some fraction of hosts is genetically very resistant to infection, there will be a shallow rise in infection as a small proportion will resist extreme doses, thus slowing the increase in infection rate at the high doses. However though this second fit does a better job in describing the overall shape of the curve, it does so by assuming an extreme variation in susceptibilities that is unlikely in our highly inbred insects. The underlying assumptions in the model imply host susceptibilities follow a beta distribution with a very high degree of heterogeneity; for instance the likelihood of infection per spore has a 95% confidence interval of $(2.55 * 10^{-4}, 1.55 * 10^{-1})$ which is unrealistically large for a highly inbred population and orders of magnitude larger than host heterogeneity when measured in a different host-pathogen system (Ben-Ami et al., 2010).

The Beta-exponential is clearly a better fit by visual inspection, and its AIC is much lower. Both models do a poor job in predicting the infection likelihood in the lowest doses. In the exponential model, the low doses are significantly underestimated, and in contrast, in the Beta-exponential the lowest dose risk is significantly overestimated. In practice, a researcher would fit a plausible model based on the data available, and then estimate risks at low doses given this best fit. However for a model to reliably predict data outside the range in which it is fitted, it ought to conform to biologically realistic assumptions. As we mention above, the host heterogeneity required in the beta-exponential is far higher than seems plausible, and more importantly the previous experiments demonstrated that the fundamental assumption of independence in both these models is questionable.

To more systematically test the impact of fitting the IAH-based Beta-exponential fit to our function we simulate the process of estimating the lowest dose (mean spores 4.65) given the top 7 points (the choice of 7 is arbitrary, but this choice does not affect the outcome of this approach). We bootstrap (resampling the data with replacement) for each dose, to come up with additional simulated experiments. For each of these simulated experiments, we estimate mortality at the lowest dose by fitting the Beta-exponential function to the top 7 doses; we then compare this to the actual mortality at this dose. We subtract the two, and plot this in figure 5. These differences are positive over 98% of the time, indicating that there is a consistent overestimation of risk at this value from extrapolating the best fit beta-exponential model from higher doses. This is consistent with mortality being very unlikely until enough toxins are in the inoculum and the likelihood of fatal infection per bacterium increasing with dose.

Incorporating cooperative toxin action

We now propose an alternative model to describe a situation where passing an initial barrier is dependent on the number of cells present. The actual dynamics of surpassing the midgut barrier involves some interaction between weakening, perforation, and healing of the host midgut, not all of which is entirely understood. So this model only represents a step toward integration of basic biological details, particularly the collective effect of released toxins, into dose-response prediction. It makes a few significant simplifications; namely it assumes that perforation is a binary state which allows either all or none of the bacteria in the midgut into the haemolymph. Our model of infection is as follows: 1) some number of bacteria are ingested by the host (k) 2) depending on the amount of toxins and the number of spores, these bacteria pass the midgut and make it to the heomolymph. 3) After this point, each bacterium has an independent probability of causing an infection, with variation due to host heterogeneity. Assuming dose is Poisson distributed this can be roughly approximated by $P(k) = \left(1 - \left(1 + \frac{k}{c_1}\right)^{-c_2}\right)\,(1 - e^{-c_3 k})$ as each bacterium carries one toxin crystal where c_1 and c_2 describe the likelihood of toxin crystals puncturing the midgut, and c_3 is the likelihood of septicaemia per cell afterward. Here we have just used the form of the Beta-exponential fit to describe toxin efficacy but any general model with diminishing shape would work; this fit is just phenomenological and does not make any assumptions on host heterogeneity nor independent action (this said, it is still incorrect if toxin action cannot be described as each toxin crystal acting independently, which is likely the case). When we get better approximations of the relative strength of toxin IBs produced by E. coli and in WT, we may be able to directly use data from toxin curves like those in figure 2. The actual mortality likelihood after midgut perforation assumes an Exponential curve, so there is no host heterogeneity assumed in this model. The best fit parameters in the model are $c_1 = 0.476, c_2 = 8.06, c_3 = 0.190$, with an AIC of 31.22 (Fig 6A). We can more formally evaluate this fit by parametric bootstrapping from this best fit using the standard error as standard deviation in the bootstrapped parameters with (mean, S.D.): $c_1 = (8.0632{,}3.36939)$, $c_2 = (0.4755, .06601), c_3 = (.1902, .0861)$. From this we can for each dose simulate data, assuming our model were true; we can then compare this to the data at these points directly resampled. Figure 6B shows the difference of these values at the low dose is no longer consistently over-estimated; bootstrapping 10,000 replicates this time leads to 20.21% below the prediction. This is repeated in Figure 6C with all doses, where the differences are plotted.

Discussion:

Here we have demonstrated the likely failure of the independent action hypothesis in the bacterial pathogen *Bacillus thuringiensis,* infecting larvae of the diamondback moth *Plutella xylostella*. In this system, the bacteria's toxin crystals must perforate the host midgut in order for bacteria to reach the insect's haemolymph. The likelihood of puncturing this midgut barrier is an increasing function of the total quantity of toxin crystals in the inoculum (figure 3). Thus when a moth is inoculated with wildtype strains, the likelihood of a given bacterium passing this midgut barrier depends on how many other cells there are in the inoculum. This midgut barrier is the primary obstacle for an invading bacterium; when this barrier is removed by inoculating the insects with enough toxins to nearly guarantee midgut perforation, the number of present spores has a remarkably weak effect on infection likelihood (figure 4). The collective action of toxins in surpassing the midgut casts doubts about the validity of the independent action hypothesis in our system, however additional experiments are required to definitively show it. Further the two most popular dose-response functions which assume IAH lead to inaccurate risk predictions at low doses.

The independent action hypothesis states "*(a)* that bacteria act independently after inoculation, and *(b)* a mean probability ($1 > p > 0$) per inoculated bacterium of initiating a fatal infection which is constant and unaffected by the number of bacteria inoculated" (Meynell, 1957). The first component has been partly challenged in recent years as microbiologists have begun to uncover the huge breadth of social interactions among many microbes (West et al., 2006). The second, which forms the basis of most current dose-response models, has been generally accepted. Though questions have been raised about the broad applicability of IAH, largely for reasons of parsimony it still forms the foundation for quantitative risk assessment in bacterial pathogens. This second component of the IAH is not, as is often implied, just the absence of an absolute threshold defining a clear minimal infective dose greater than one. Any increasing likelihood of puncturing the midgut with dose violate IAH assumptions, whether or not there exists a strict threshold. As we have stated, our data do not rule out the possibility that the toxins themselves follow independent action assumptions and that spore doses are irrelevant for mortality at low doses. If these are both true, then the second part of the IAH may not fail in our system. In order to more definitively refute the IAH, one could either demonstrate that the effect of toxins does not follow independence assumptions or that the numbers of spores at low doses impact mortality.

The dose-response curve in our system rises fast after some lag and then the increase slows down in the high doses. A similar saturation at high doses was shown previously in a bacterial parasite of Daphnia which was attributed to either host variation in susceptibility or antagonism among infecting bacteria (Regoes et al., 2003). Our data with constant spores and variable toxins (figure 2) suggests the effect is largely driven by the basic interaction between the toxin molecules and midgut. We cannot entirely rule out host heterogeneity in contributing to this effect, but the degree of variation in susceptibility necessary to explain the shape is very unlikely in our host population (inbred for over 100 generations); the beta-exponential parameters that best fits the data (shown in figure 2) implies the range of susceptibilities is $(2.55 * 10^{-4}, 1.55 * 10^{-1})$ which is unrealistically high in an inbred system. Also, and perhaps more importantly, our curve diverges from both the exponential and beta-exponential fits at the lowest doses (at doses of approximately 5 and 10, for instance).

There have been several indirect tests of the independent action hypothesis, fitting available data to the standard dose-response models. Perhaps more compelling are experiments that analyse the rate of coinfection of differentially tagged strains at low doses, where a prevalence of singly infections is implies that only the progeny from one inoculated cell is recovered from the final systemic infection (Meynell, 1957; Moxon and Murphy, 1978; Rubin, 1987). Unfortunately these tests can misdiagnose strong bottlenecks at any infection barrier as independent action throughout the infection (for instance recently demonstrated in *B. anthracis* (Plaut et al., 2012)). More convincing is an elegant extension in a virus-insect system which formalizes a simple 'null model' for infection, then varies inoculum size of each of two tagged lineages (Zwart et al., 2009). This approach is less likely to misidentify bottlenecks as support for independent action since strong bottlenecks, even with high doses of the two strains, would always yield clonal isolates in late infection. Among six virus-insect systems tested, two were consistent with IAH predictions, and four were not. As their approach was statistical rather than mechanistic, the causes of these deviations from IAH predictions are not known.

We have demonstrated that the IAH is dubious in our system, and likely as a result typical dose-response models fail, but how common might be in other pathogens? Many serious human pathogenic bacteria freely release toxins. For instance, anthrax toxins, Shiga toxin, diphtheria toxin, cholera toxin, Clostridium spp. exotoxins, pneumolysin, botulinum toxin, pertussis toxin, Staphylococcus alpha toxin, and tetanus toxin are all freely released and benefit neighbouring infecting cells (Prescott, 2002). It has been previously argued that there might be mechanism-based rules governing broad trends in median dose-responses (see (Gama et al., 2012; Leggett et al., 2012; Schmid-Hempel and Frank, 2007)). Here we extend the appeal for a mechanistic focus in dose-response to understanding the shapes of the dose-response curves. In this paper we have concentrated our efforts on shared toxins, however there are other social interactions that could have major effects on dose-responses. Many bacteria release extracellular enzymes that perform many other functions including immune cell evasion, cell-to-cell signalling (i.e. quorum sensing), and biofilm formation, which should all influence the shape of the dose-response.

Due to collective secretions, current dose-response curves are inapplicable in some organisms. Fitting an IAH model to a system that infects collectively could overestimate low dose risks because the parameters being fit have little to do with the underlying biology. From a public health perspective, this can mean a misallocation of resources from one target to another. These methods are also recommended in response to bioterrorism attacks (Canter, 2005; National Research Council, 2005) and in fact a charge against the handling of the 2001 anthrax scare in the United States was that risk was grossly overestimated, costing millions in unnecessary sterilization due to not incorporating threshold effects into the models (Coleman et al., 2008; Loving et al., 2009). Outside of analysing data for risk assessment, cooperative infections can have significant impact by causing an invasion threshold (Regoes et al., 2003). In addition, the validity of IAH is of great importance to those trying to understand genetic drift and within-host interactions of various populations (Zwart et al., 2011).

The articulation of the independent action hypothesis more than fifty years ago has been helpful to clarify thoughts on infection biology and risk. But the biology that has been uncovered in the years since questions its generality. The standard models of dose response make assumptions on the interactions of infecting bacteria that are difficult to justify biologically in many pathogens. For this reason even where statistical fits based on these bad assumptions are good in some intervals, they can falter in the untested interval that matters most, the low doses. The question of how many pathogen cells are required to cause infection is one of the most basic questions that can be asked about pathogenesis, and biological mechanism must be carefully considered to answer it.

Experimental methods: (this section was written by Ben Raymond)

Spontaneous antibiotic resistance mutants of *B. thuringienis kurstaki* HD-1, were isolated from the commercial biopesticide preparation, DiPel WP (Valent Biosciences), by plating high densities of cells (10^8+) 15 µg ml-1 nalidixic acid. An antibiotic resistant mutant with reduced fitness cost (6G NalR) was isolated after a round of host passage in *P. xylostella* (Garbutt et al., 2011), and identified by rapid growth on selective plates. This strain was cured of its Cry toxin producing plasmid by growth at high temperature (42 °C) and isolating colonies with unusual morphology at sporulation and in order to produce the isolate Cry null 6.20 NalR. Absence of Cry toxin production was confirmed by microscopy and bioassays with *P. xylostella*. Sporulated cultures of all strains were produced by growing dense lawns of bacteria on HCO sporulation media (Lecadet et al., 1980) at 30°C for 1 week. Spores and Cry toxins were recovered from plates and washed twice in sterile saline (0.85% NaCl), before being diluted into 10ml of saline and stored at -20°C in 0.5 ml aliquots for up to 8 weeks. Defrosted spores were enumerated by plating serial dilutions; replicated counts were made within 48 hours of infecting insects. Exogenous Bt Cry toxin (Cry1Ac) was produced in Escherichia coli JM109 cells carrying the plasmid pGem1Ac, a gift of Dr Neil Crickmore (University of Sussex). Cells were grown in 500ml of double strength LB for 3 days at 37°C with 100 μg ml-1 ampicillin. After centrifugation (6000 g) pellets were suspended in 30 ml sterile de-ionized water and sonicated in 15ml aliquots using a Branson sonicator at 25% amplitude with four bursts of 40s with 40s rests on ice between each burst. Cells were centrifuged at 5000 g before being resuspended in water with 0.5% Triton X-100 before an additional minute of sonication. Cells were then centrifuged, and resuspended one more time before stored at -20°C in 1ml aliquots. Total Cry toxin production was estimated using SDS-PAGE and densitometry with BSA as standard using the Biorad Image Lab 4.01 software. Toxin aliquots were pasteurized (heat treated at 65°C for 20 minutes) before use in bioassays in order to kill any remaining *E. coli* cells.

An inbred population of *P. xylostella* larvae (Geneva 88) were reared on artificial diet (without antibiotics) as described previously (Raymond et al., 2009), this population has been in continuous culture for at least 20 years (Shelton et al., 1991). Early third instars were infected with Bt in droplet assays. The final droplet mix contained 10mM sucrose, 7.5% v/v green food dye (Dr Oetker, www.oekter.co.uk) and 0.4% w/v agar (Oxoid Bacteriological), and 40% v/v cabbage extract (filtered liquid from boiled cabbages). The cabbage juice, sucrose and food dye were filter sterilized before being used to dilute the spores; this mixture was then combined (50:50) with molten 0.8% agar (at 60 °C). The resultant inoculum (with a final concentration of 300 cfu μl^{-1}) was briefly held at 50°C in heat block while 1μl droplets were dispensed into each well of 48 well plates using prewarmed pipette tips. A single larva was added to each well, and plates were tightly sealed with damp tissue paper: larvae were allowed to feed for up to 18 hours. After feeding, larvae that had consumed droplets, and which had visible green dye throughout their intestinal tract, were transferred to artificial diet for 5 days. Successful infections were classed as larvae that died and produced the strongly melanised cadavers indicative of Bt infection.

We carried out three sets of droplet bio-assays in order to test the IAH The first set aimed to accurately establish the shape of the dose response curve to *B. t. kurstaki* HD-1 spores and toxins using P1G NalR. Assays used ten doses based on a two-fold dilution series starting at 2400 CFU with an additional saline control. This assay was repeated five times, each replicate was initiated with 24 larvae per dose. On average 21/24 larvae per dose were judged to have consumed their droplets satisfactorily and were included in the final assay analysis. The second group of assays aimed to explore the effect of increasing concentrations of the public good virulence factor (exogenous Cry1Ac toxin) while holding the spore dose constant (using Cry null 6.20 NalR). This experiment used a constant spore dose of 900 CFU, while toxin dose varied from 5 pg to 23 ng; this assay was repeated twice and set up with 48 larvae per dose in each replicate. The final set of assays measured the response of mortality to variation in spore dose (using Cry null 6.20 NalR) while holding the dose of exogenous Cry1Ac constant. This experiment was carried out at two doses of exogenous toxin (60 or 180 pg Cry1Ac) and was set up with 48 larvae per dose.

Artiola, J.F., Pepper, I.L., Brusseau, M.L., 2004. Environmental Monitoring and Characterization. Academic Press.

Ben-Ami, F., Ebert, D., Regoes, R.R., 2010. Pathogen Dose Infectivity Curves as a Method to Analyze the Distribution of Host Susceptibility: A Quantitative Assessment of

Maternal Effects after Food Stress and Pathogen Exposure. The American Naturalist 175, 106–115.

Ben-Ami, F., Regoes, R.R., Ebert, D., 2008. A quantitative test of the relationship between parasite dose and infection probability across different host-parasite combinations. Proc. Biol. Sci. 275, 853–859.

Buchanan, R.L., Havelaar, A.H., Smith, M.A., Whiting, R.C., Julien, E., 2009. The Key Events Dose-Response Framework: Its Potential for Application to Foodborne Pathogenic Microorganisms. Crit Rev Food Sci Nutr 49, 718–728.

Canter, D.A., 2005. Addressing Residual Risk Issues at Anthrax Cleanups: How Clean is Safe? Journal of Toxicology and Environmental Health, Part A 68, 1017–1032.

Coleman, M.E., Thran, B., Morse, S.S., Hugh-Jones, M., Massulik, S., 2008. Inhalation anthrax: dose response and risk analysis. Biosecur Bioterror 6, 147–160.

Cox, L.A., 2006. Dose-Response Modeling and Risk Characterization, in: Hillier, F.S. (Ed.), Quantitative Health Risk Analysis Methods, International Series in Operations Research & Management Science. Springer US, pp. 169–223.

Druett, H.A., 1952. Bacterial Invasion. Nature, Published online: 16 August 1952; | doi:10.1038/170288a0 170, 288–288.

Fazil, A.M., 2005. A Primer on Risk Assessment Modelling: Focus on Seafood Products. Food & Agriculture Org.

Fryer, H.R., McLean, A.R., 2011. There Is No Safe Dose of Prions. PLoS ONE 6, e23664.

Gama, J.A., Abby, S.S., Vieira-Silva, S., Dionisio, F., Rocha, E.P.C., 2012. Immune Subversion and Quorum-Sensing Shape the Variation in Infectious Dose among Bacterial Pathogens. PLoS Pathog 8, e1002503.

Garbutt, J., Bonsall, M.B., Wright, D.J., Raymond, B., 2011. Antagonistic competition moderates virulence in Bacillus thuringiensis. Ecology letters 14, 765–772.

Haas, C.N., Rose, J.B., Gerba, C.P., 1999. Quantitative Microbial Risk Assessment. John Wiley and Sons.

Haas, C.N., Thayyar-Madabusi, A., Rose, J.B., Gerba, C.P., 2000. Development of a dose-response relationship for Escherichia coli O157:H7. International Journal of Food Microbiology 56, 153–159.

Hazard Characterization for Pathogens in Food and Water: Guidelines, 3rd ed, 2004. . Food & Agriculture Organization.

Lecadet, M.M., Blondel, M.O., Ribier, J., 1980. Generalized transduction in Bacillus thuringiensis var. berliner 1715 using bacteriophage CP-54Ber. J. Gen. Microbiol. 121, 203–212.

Leggett, H.C., Cornwallis, C.K., West, S.A., 2012. Mechanisms of Pathogenesis, Infective Dose and Virulence in Human Parasites. PLoS Pathog 8, e1002512.

Loving, C.L., Khurana, T., Osorio, M., Lee, G.M., Kelly, V.K., Stibitz, S., Merkel, T.J., 2009. Role of anthrax toxins in dissemination, disease progression, and induction of protective adaptive immunity in the mouse aerosol challenge model. Infect. Immun. 77, 255–265.

Meynell, G.G., 1957. The Applicability of the Hypothesis of Independent Action to Fatal Infections in Mice given Salmonella typhimurium by Mouth. J Gen Microbiol 16, 396–404.

Moxon, E.R., Murphy, P.A., 1978. Haemophilus influenzae bacteremia and meningitis resulting from survival of a single organism. Proc Natl Acad Sci U S A 75, 1534–1536.

National Research Council, 2005. Reopening Public Facilities After a Biological Attack: A Decision-Making Framework. National Academies Press.

Plaut, R.D., Kelly, V.K., Lee, G.M., Stibitz, S., Merkel, T.J., 2012. Dissemination Bottleneck in a Murine Model of Inhalational Anthrax. Infect. Immun. 80, 3189–3193.

Prescott, L.M., 2002. Microbiology, Fifth Edition, 5th ed. McGraw-Hill Science/Engineering/Math.

Raymond, B., Johnston, P.R., Nielsen-LeRoux, C., Lereclus, D., Crickmore, N., 2010. Bacillus thuringiensis: an impotent pathogen? Trends in Microbiology 18, 189–194.

Raymond, B., Johnston, P.R., Wright, D.J., Ellis, R.J., Crickmore, N., Bonsall, M.B., 2009. A mid-gut microbiota is not required for the pathogenicity of Bacillus thuringiensis to diamondback moth larvae. Environ. Microbiol. 11, 2556–2563.

Raymond, B., West, S.A., Griffin, A.S., Bonsall, M.B., 2012. The Dynamics of Cooperative Bacterial Virulence in the Field. Science 337, 85–88.

Regoes, R.R., Hottinger, J.W., Sygnarski, L., Ebert, D., 2003. The infection rate of Daphnia magna by Pasteuria ramosa conforms with the mass-action principle. Epidemiol Infect 131, 957–966.

Ridout, M.S., Fenlon, J.S., Hughes, P.R., 1993. A generalized one-hit model for bioassays of insect viruses. Biometrics 1136–1141.

Rubin, L.G., 1987. Bacterial Colonization and Infection Resulting from Multiplication of a Single Organism. Clin Infect Dis. 9, 488–493.

Schmid-Hempel, P., Frank, S.A., 2007. Pathogenesis, Virulence, and Infective Dose. PLoS Pathog 3, e147.

Schnepf, E., Crickmore, N., Rie, J.V., Lereclus, D., Baum, J., Feitelson, J., Zeigler, D.R., Dean, D.H., 1998. Bacillus thuringiensis and Its Pesticidal Crystal Proteins. Microbiol. Mol. Biol. Rev. 62, 775–806.

Shelton, A.M., Cooley, R.J., Kroening, M.K., Wilsey, W.T., Eigenbrode, S.D., 1991. Comparative analysis of two rearing procedures for diamond-back moth (Lepidoptera: Plutellidae). Journal of Entomological Science 26.

West, S.A., Griffin, A.S., Gardner, A., Diggle, S.P., 2006. Social evolution theory for microorganisms. Nature Reviews Microbiology 4, 597–607.

Westcot, D.W., 1997. Quality control of wastewater for irrigated crop production (Water reports-10). Food and Agriculture Organization of the United Nations, Rome, Italy.

Zwart, M.P., Daròs, J.-A., Elena, S.F., 2011. One Is Enough: In Vivo Effective Population Size Is Dose-Dependent for a Plant RNA Virus. PLoS Pathog 7, e1002122.

Zwart, M.P., Hemerik, L., Cory, J.S., Visser, J.A.G.M. de, Bianchi, F.J.J.A., Oers, M.M.V., Vlak, J.M., Hoekstra, R.F., Werf, W.V. der, 2009. An experimental test of the independent action hypothesis in virus–insect pathosystems. Proc. R. Soc. B 276, 2233–2242.

Figure 1: Two scenarios showing bacteria crossing two barriers to fatal infection inside the host. In the first scenario, both barriers are independent-action, meaning that every bacterium has some probability of passing each barrier, independent of others around it. In the second scenario, the first barrier is surpassed by a collective process (in this case release of toxins), and the subsequent barrier is passed independently. This second scenario is inconsistent with independent action assumptions because the likelihood that a particular bacterium will cross all barriers depends on other cells in the inoculum as this affects success in passing the first one.

Figure 2: A) The mortality rates for 900 *Bacillus thuringiensis* spores supplemented with varying quantities of toxins. Two blocks of data are shown (blocks differentiated by shape). B) The same data but only low doses and at a linear scale. Data points comes from two sets of experiments with 48 insects at each dose; the first block includes all doses shown from 74.22 to 38,000, and the second block includes doses from 9.28 to 9500, and both blocks include the dose of 0.

Figure 3: The mortality rates for *Bacillus thuringiensis* knockouts supplemented with 100 IBs (triangles) and 300 IBs (circles). Data points come from two sets of experiments, one at each of the two toxin doses. Both experiments were initiated with 48 insects each for each dose.

Figure 4: The dose-response for wildtype *Bacillus thuringiensis* with 95% confidence intervals. Also drawn are the independent action curves fit; the exponential fit (p=0.006226; AIC=230.9641) and the Beta-exponential (α=0.5374, β=12.1732, AIC = 32.72). Data points here are means from five blocks of experiments, each initiated with 24 insects.

Figure 5: The distribution of the difference between predicted infection rate from best-fit beta-exponential model (fit to the top seven data points) at mean dose 4.65 and the actual rate among simulated experiments (bootstrapping data from each dose 10,000 times). The difference is positive 98.04% of the time with a mean of 0.094, indicating that the beta-exponential fit overestimates risk consistently, estimating mortality rate to be on average 15.96% compared to the directly resampled mean at this dose of 9.39%.

Figure 6: A) The fit of a model that incorporates a cooperative step of infection ($c_1 = 0.476, c_2 = 8.06, c_3 = 0.190$, AIC = 31.22), compared to the best fit Beta-exponential model (α=0.5374, β=12.1732, AIC = 32.72). B) The difference between estimations of the lowest dose from parametric bootstrapping and from direct resampling of this data. Consistent over or underestimations will be shown as deviations from a difference of zero. Here however, there is no consistent over or underestimations of this value. C) The difference between the parametric and nonparametric bootstrap values for predictions at each dose, showing no dose is consistently over or under estimated. Dashed lines are at 0.05 and 0.95.

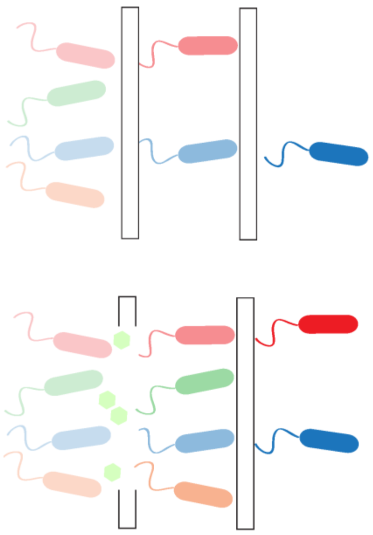

Figure 1

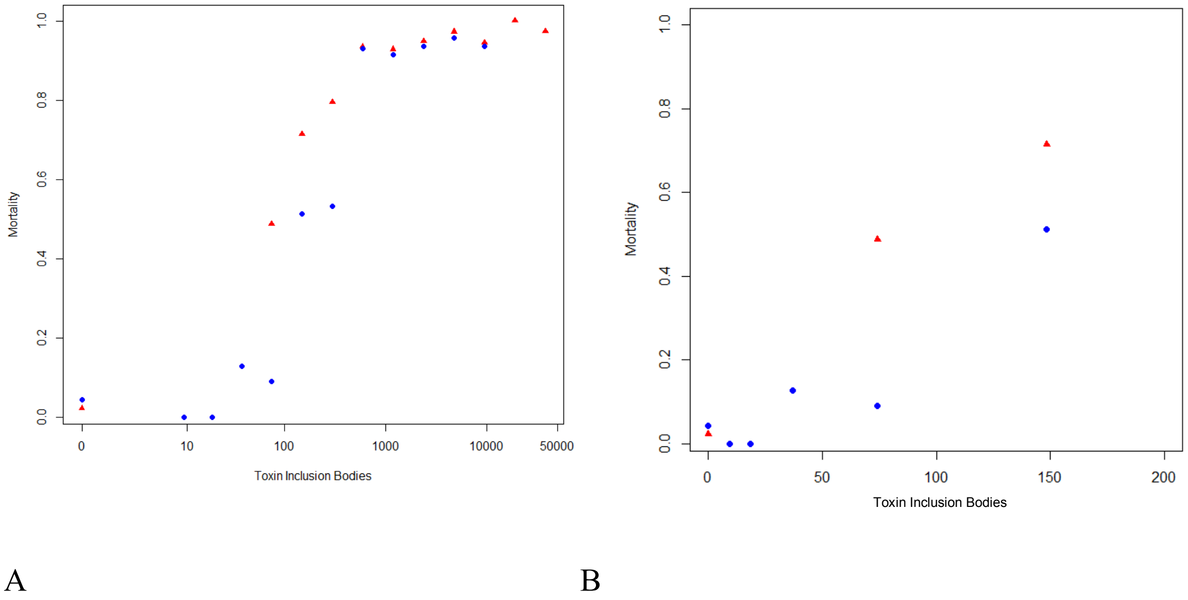

Figure 2

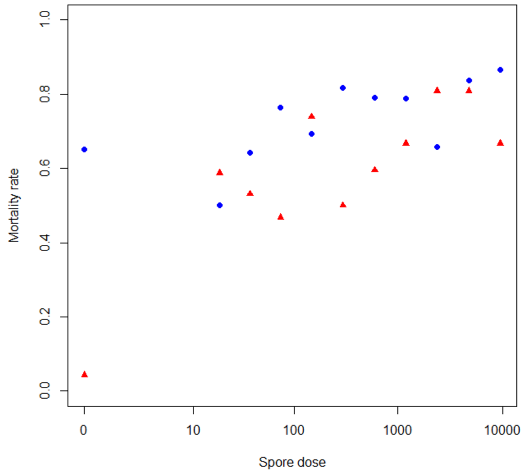

Figure 3

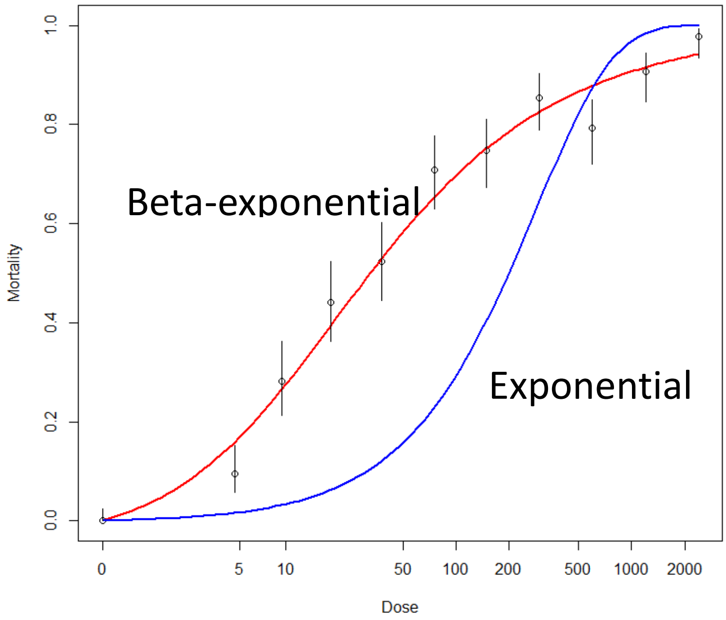

Beta-exponential
Exponential
Mortality
0.0
0.2
0.4
0.6
0.8
1.0
Dose
0
5
10
50
100
200
500
1000
2000

Figure 4

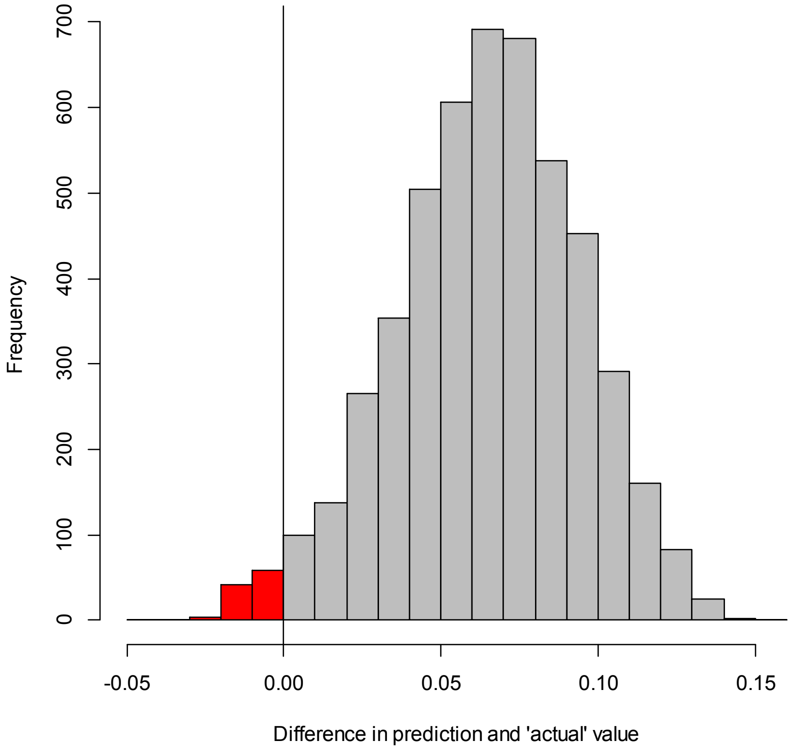
Frequency
0
100
200
300
400
500
600
700
-0.05
0.00
0.05
0.10
0.15
Difference in prediction and 'actual' value

Figure 5

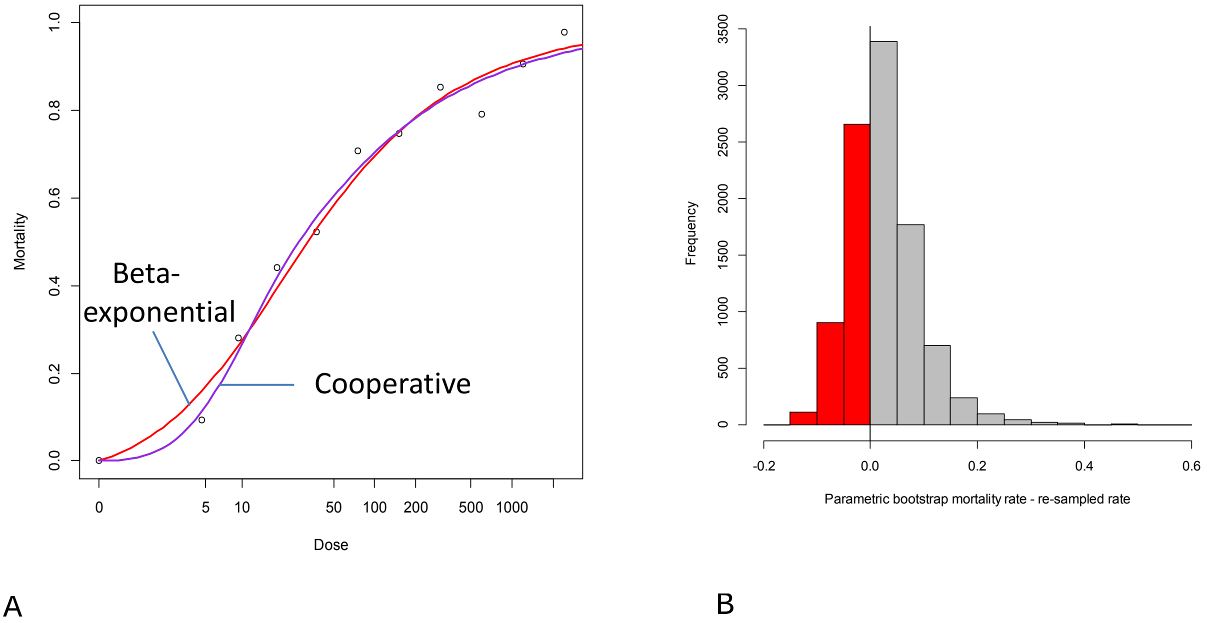
Mortality
0.0
0.2
0.4
0.6
0.8
1.0
Beta-
exponential
Cooperative
0
5
10
50
100
200
500
1000
Dose
Frequency
0
500
1000
1500
2000
2500
3000
3500
-0.2
0.0
0.2
0.4
0.6
Parametric bootstrap mortality rate - re-sampled rate

A

B

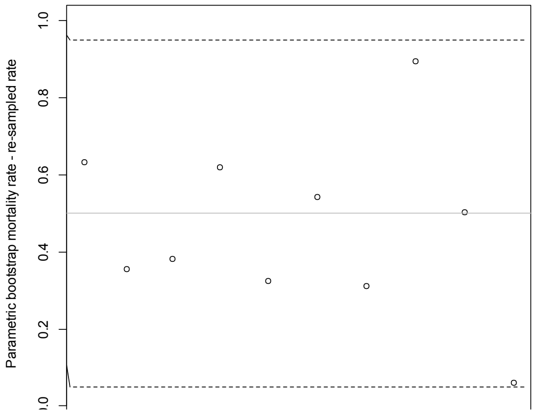
Parametric bootstrap mortality rate - re-sampled rate
1.0
0.8
0.6
0.4
0.2

C

Figure 6